J Neurophysiol 89: 276–289, 2003;
10.1152/jn.00159.2001.

Coordinated Turn-and-Reach Movements. I. Anticipatory Compensation for Self-Generated Coriolis and Interaction Torques

PASCALE PIGEON, SIMONE B. BORTOLAMI, PAUL DIZIO, AND JAMES R. LACKNER
Ashton Graybiel Spatial Orientation Laboratory, Brandeis University, Waltham, Massachusetts 02454-9110

Submitted 26 February 2001; accepted in final form 13 June 2002

Pigeon, Pascale, Simone B. Bortolami, Paul DiZio, and James R. Lackner. Coordinated turn-and-reach movements. I. Anticipatory compensation for self-generated Coriolis and interaction torques. *J Neurophysiol* 89: 276–289, 2003; 10.1152/jn.00159.2001. When reaching movements involve simultaneous trunk rotation, additional interaction torques are generated on the arm that are absent when the trunk is stable. To explore whether the CNS compensates for such self-generated interaction torques, we recorded hand trajectories in reaching tasks involving various amplitudes and velocities of arm extension and trunk rotation. Subjects pointed to three targets on a surface slightly above waist level. Two of the target locations were chosen so that a similar arm configuration relative to the trunk would be required for reaching to them, one of these targets requiring substantial trunk rotation, the other very little. Significant trunk rotation was necessary to reach the third target, but the arm's radial distance to the body remained virtually unchanged. Subjects reached at two speeds—a natural pace (slow) and rapidly (fast)—under normal lighting and in total darkness. Trunk angular velocity and finger velocity relative to the trunk were higher in the fast conditions but were not affected by the presence or absence of vision. Peak trunk velocity increased with increasing trunk rotation up to a maximum of 200°/s. In slow movements, peak finger velocity relative to the trunk was smaller when trunk rotation was necessary to reach the targets. In fast movements, peak finger velocity was ~1.7 m/s for all targets. Finger trajectories were more curved when reaching movements involved substantial trunk rotation; however, the terminal errors and the maximal deviation of the trajectory from a straight line were comparable in slow and fast movements. This pattern indicates that the larger Coriolis, centripetal, and inertial interaction torques generated during rapid reaches were compensated by additional joint torques. Trajectory characteristics did not vary with the presence or absence of vision, indicating that visual feedback was unnecessary for anticipatory compensations. In all reaches involving trunk rotation, the finger movement generally occurred entirely during the trunk movement, indicating that the CNS did not minimize Coriolis forces incumbent on trunk rotation by sequencing the arm and trunk motions into a turn followed by a reach. A simplified model of the arm/trunk system revealed that additional interaction torques generated on the arm during voluntary turning and reaching were equivalent to $\leq 1.8\ g$ ($1\ g = 9.81\ m/s^2$) of external force at the elbow but did not degrade performance. In slow-rotation room studies involving reaching movements during passive rotation, Coriolis forces as small as $0.2\ g$ greatly deflect movement trajectories and endpoints. We conclude that compensatory motor innervations are engaged in a predictive fashion to counteract impending self-generated interaction torques during voluntary reaching movements.

INTRODUCTION

Arm movements made within a rotating reference frame generate Coriolis forces that are a function of the cross product of the angular rotation of the reference frame, the linear velocity of the arm relative to the reference frame, and the effective mass of the arm.[1] Because Coriolis forces are proportional to limb velocity, they are absent prior to and after a movement, but their impact on movement trajectory can be substantial if the nervous system does not account for them. For example, subjects seated at the center of a fully enclosed slow-rotation room (SRR) turning at constant velocity have their initial reaching movements to targets deflected from their intended paths and endpoints in the direction of the Coriolis forces generated on the arm. With repeated movements, even without visual feedback, subjects adapt and their movements regain straight trajectories and accurate endpoints (DiZio and Lackner 2000; Lackner and DiZio 1994).

In nonrotating environments, joint torques due to Coriolis forces arise whenever two or more joints of the same limb or mechanical linkage move simultaneously. For example, when the elbow extends while the shoulder flexes, a Coriolis torque emerges at the shoulder. Similarly, when the trunk turns as the arm is extended away from the body in a reaching movement, the trunk serves as a rotating reference frame within which the arm moves, thereby generating additional Coriolis torques at the arm joints. Besides Coriolis torques, the dynamic interaction between the trunk and the moving segments of the arm also gives rise to additional centripetal and inertial torques, collectively known as interaction torques.

Interaction torques are significant during multijoint arm reaching movements even without trunk rotation (Hollerbach and Flash 1982). Despite this potentially disturbing influence in reaching tasks, straight-line hand paths are typical of arm reaching movements (Abend et al. 1982; Gordon et al. 1994b; Morasso 1981). The nervous system may take interaction torques into consideration when preparing a movement involving simultaneous multijoint rotations or, alternatively, may correct trajectory deflections during movement execution. In fast reaching movements (<500 ms), neuronal loop delays may prohibit trajectory corrections based on current visual or

[1] $F_{cor} = -2M(\omega \times v)$, where M is the mass of the arm, ω is the velocity of room rotation in radians/s, and v is the velocity of the arm in m/s.

Address for reprint requests: P. Pigeon, Ashton Graybiel Spatial Orientation Laboratory, MS 033, Brandeis University, P.O. Box 549110, Waltham, MA 02454-9110 (E-mail: pigeon@brandeis.edu).

The costs of publication of this article were defrayed in part by the payment of page charges. The article must therefore be hereby marked "*advertisement*" in accordance with 18 U.S.C. Section 1734 solely to indicate this fact.

proprioceptive feedback, suggesting that a mostly predictive, open-loop form of control may underlie the compensation of interaction torques (Gribble and Ostry 1999).

Straight-line hand paths, in addition to implying compensation for interaction torques in multijoint movements, are consistent with the hypothesis that reaching movements are planned in end effector coordinates (Flash and Hogan 1985; Morasso 1981). Theoretically, the coordinate system may be coupled to external (extrapersonal) space, its origin coinciding with hand position prior to the arm movement (Gordon et al. 1994b), or the coordinate system may be coupled to the body with its origin located, for example, on the trunk. When trunk motion is negligible during a reaching task or involves only translation in the sagittal plane to shift the hand toward the target (Kaminski et al. 1995; Saling et al. 1996), typical features of hand trajectories in external space such as straight-line paths and bell-shaped velocity profiles may be preserved when the trajectory is observed from a trunk-based frame of reference (Wang and Stelmach 1998). However, based on data involving only linear trunk motion, it cannot be inferred whether movement planning occurs in external or body relative coordinates. Examining the hand paths and velocity profiles of reaching movements produced in combination with trunk *rotation* may provide insights into whether reaching movements are planned in external or trunk-based frames of reference.

This paper is the first of a series in which we describe both the kinematic and dynamic features of reaching movements produced with and without voluntary trunk rotation. In the paradigm we employed, subjects standing in front of a table slightly above waist level pointed to each of three visual targets. For two of the targets, a similar arm configuration relative to the trunk was required for reaching the targets, but one required substantial leftward trunk rotation and the other very little. To reach the third target, significant trunk rotation was required, but the arm was kept at approximately the same radial distance to the body. The different coordination requirements between the trunk and arm for each target allowed us to contrast reaching movements produced with a variety of trunk-motion-induced torques.

Our first goal was to determine whether arm-reaching movements involve compensation for interaction torques induced by self-generated trunk rotation. The trajectory characteristics and accuracy of reaching movements produced with trunk rotation were compared with those of reaching movements involving minimal trunk motion. We analyzed the timing between the arm and trunk movements in reaches involving significant trunk rotation to test the hypothesis that the CNS may minimize Coriolis torques by sequencing the motion of the arm and trunk segments. At the shoulder and elbow joints, such a strategy would eliminate trunk-motion-induced Coriolis torques during the entire reach but would still require active compensation of the centripetal and inertial interaction torques resulting from trunk motion. Because interaction torques induced by trunk rotation scale with the speed of the trunk and arm movements, we had subjects produce reaching movements at a natural pace as well as rapidly. This allowed us to assess the effect of reaching velocity on the shape and accuracy of the hand trajectory as well as on the trunk rotation and arm joint angles during the movements and to examine whether increasing the dynamical demands of the task altered the pattern of interjoint coordination. Specifically, we sought to determine whether differences in arm-trunk coordination and/or hand trajectory between slower and faster reaches could be explained by a variation in the magnitude of trunk-rotation–induced torques. To examine the possible role of visual feedback in compensating interaction torques due to trunk rotation at both the hand trajectory and joint angle levels, we had subjects produce movements in normal lighting conditions and in dark conditions in which only the target light was visible prior to the reaching movement.

The present paper describes several findings related to the compensation of interaction torques, including the accuracy of reaching movements for conditions involving different magnitudes of trunk-rotation–induced torques, the contribution of visual feedback to performance, and the sequencing of hand and torso motion. In addition, as a first step toward a detailed inverse dynamics analysis of turn-and-reach movements, a simplified model of the arm/trunk system is used to estimate the size and direction of the interaction torques at the arm joints and to assess their expected effects on the reaching movements if not appropriately compensated. The effect of reaching velocity and of interaction torque magnitude on the trajectory pattern and interjoint coordination pattern of reaches is discussed in the companion paper (Pigeon et al. 2003). This paper also addresses the second goal of these experiments, the investigation of the frame of reference in which reaching movements combining arm extension and trunk rotation are planned. Finally, an upcoming paper will present an in-depth inverse dynamics analysis of the movements generated during turn-and-reach maneuvers and describe the associated muscle torques (Bortolami et al. 1999; unpublished data). The general conclusion of all three papers is that the CNS anticipates and compensates for the interaction torques generated during natural turning and reaching activities.

Some of the results reported here were presented in preliminary form at the Society for Neuroscience annual meeting in 1999 (Pigeon et al., 1999).

METHODS

Subjects

Five male and two female subjects (ages, 19–55 yr) with no known musculoskeletal or neurological disorders participated. Each subject signed a consent form outlining the procedures approved by the Institutional Review Board at Brandeis University.

Apparatus

The subject stood in a semicircular cutout section of a table (Fig. 1). To minimize leaning of the trunk above the workspace surface, the height of the table was adjusted for each subject's height and arm length until the shoulder to table distance was in a 29- to 39-cm range (mean: 33.4 cm). Three light-emitting diodes (LEDs) inlaid in the surface of the table were used as targets. Pointing movements were initiated from a microswitch that controlled the illumination of the LEDs. The microswitch provided a start position that was near the subject and aligned with the sagittal midline of the trunk. When the finger was positioned above the microswitch prior to a movement, the upper arm was abducted ~40°.

The target and microswitch locations were defined using a polar coordinate system the origin of which coincided with the center of the cutout section where the subjects stood. A line bisecting the semicircular section marked the 0° direction and indicated the direction the subject faced at the beginning of each trial. The microswitch was located along this direction, 25 cm from the origin.

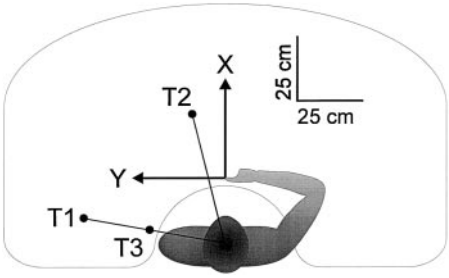

FIG. 1. Experimental setup. The locations of the start position and of the 3 light-emitting diodes used as targets (T1, T2, T3) were defined relative to a polar coordinate system originating at the center of the table cut-out section. Reaching movements were recorded relative to a Cartesian coordinate system originating at the start position of the finger.

The three targets were located on the left side of the table in positions designed to involve different amounts of arm extension and trunk rotation. Pointing to target 1 (T1) required both arm extension and trunk rotation to move the hand to the left side of the table and away from the torso. Pointing to target 2 (T2) required approximately the same arm extension used in pointing to T1 but without the trunk rotation. Pointing to target 3 (T3) required maintaining the hand's initial radial distance from the torso while moving it through a similar angular displacement as when pointing to T1.

The target positions were defined in the polar coordinate system as follows. T1 was located 80° to the left of the forward direction, 54.8 cm from the center of the cutout section. To identify the location of T2, subjects were asked to make a pointing movement to T1 using their right arm and to maintain their final arm and trunk positions. Then while grasping their right wrist with their left hand to keep the configuration of the right arm as constant as possible and with their right index finger slightly above the table surface, they slowly rotated their trunk back to its initial position. When the initial trunk position had been regained, they dropped their index onto the table and this position was noted. Six measurements were taken for six subjects. The resulting average position for T2 across subjects was 54.3 cm from the origin, a radial distance virtually identical to that of T1 (thus confirming that the maneuver removed the trunk rotation component of the reaching movement), and 14° to the left of the forward direction. Finally, T3 was placed along the same angular direction as T1 (80° to the left), 25 cm from the origin to match the radial distance of the finger when poised above the microswitch prior to a pointing movement.

The (straight-line) reaching distances to T1–T3 were 56.1, 30.6, and 32.2 cm, respectively. Subjects used ~88° of elbow extension, 77° of shoulder flexion, and 60° of trunk rotation to reach T1. The corresponding joint rotations used to reach the other targets were respectively 83, 62**,** and 9° for T2 and 22, 48, and 39° for T3. In addition, subjects increased shoulder abduction by ~12° to reach T1 and 8° to reach T2, with very little change in abduction to reach T3.

Experimental procedures

Each trial started with the subject standing at the table with the right arm resting on its surface. In response to an auditory signal, the subject lifted the arm slightly above the table and depressed the microswitch with the right index finger, thereby illuminating one of the LEDs. The subject looked at the target and, when confident of its position, returned the head and eyes back to the hand at the start position and then reached to touch the target with the index finger in one smooth natural motion. Lifting the index finger off the microswitch turned off the LED. A smooth panel of transparent Plexiglas covered the table and LEDs so that the subject touched down without receiving direct tactile feedback about the accuracy of the pointing movement. The subject maintained the hand and head in the final position until instructed by the experimenter to return to the start position. The subject could extend the arm and turn the trunk to reach a target but was asked not to move the feet or lean toward the target. Although these latter problems could have been alleviated by having subjects sit at the experimental table, standing subjects could produce larger trunk rotation amplitudes (with contributions from rotational degrees of freedom in the torso, hip, and leg) in combination with the arm reaching movements.

The reaching movements were produced in four experimental conditions during a single experimental session: light-slow (LS), light-fast (LF), dark-slow (DS), and dark-fast (DF). The order of the experimental conditions was randomized across subjects. In the light conditions, the room was illuminated normally and the location of the targets was visible even when the LEDs were off. In the dark conditions, only the target lights were visible; thus after lifting the finger off the microswitch, the subject was reaching to the remembered position of the target. In the slow conditions, the subject was instructed to reach at a movement speed comparable to that used to reach and pick up a fork, whereas in the fast condition, to that required to trap a fly sitting on the table. The subject was allowed several practice trials until the experimenter was satisfied that the correct speed for slow and fast movements had been achieved.

Each subject was assigned a random sequence of nine movements involving three trials to each target (e.g., T3, T1, T2, T2, T2, T1, T3, T3, T1). The subject repeated this sequence of movements three times in one experimental condition (i.e., 27 movements) before moving on to a different condition (108 movements in total).

Data recording

Infrared LEDs were affixed to the tip of the right index finger, the styloid process of the ulna (wrist), the lateral epicondyle (elbow), the left and right acromion processes (left and right shoulders), the sternal notch (sternum), and above the left and right eyes. Three-dimensional kinematic data were recorded at 200 Hz with an Optotrak motion recording system.

In the dark conditions, the room lights remained off between trials so that the subject returned the finger to its initial position above the microswitch after each movement relying on touch and proprioception, which all subjects did without difficulty. The subject was also instructed to keep the initial body position as constant as possible between trials.

Data analysis

Variables characterizing the shape of the finger trajectory, reaching accuracy, and timing of the finger and trunk movements were analyzed. Because the reaching movements were not restricted to a plane, some vertical displacement of the arm did occur. However, this component was small compared with the horizontal component of the movement (average maximal vertical displacement of finger: 7.3, 5.3, and 5.2 cm for T1, T2, and T3, respectively). Therefore the finger trajectory was analyzed based on its two-dimensional projection on the plane of the table.

The shape of the finger trajectory was estimated by its maximal deviation, calculated in each trial in each experimental condition by finding the greatest perpendicular distance between the trajectory and the straight line joining its endpoints. This distance was considered positive for a rightward deviation and negative for a leftward deviation.

The accuracy of the reaching movements was evaluated by measuring the radial and angular pointing errors in each trial. The radial error was defined as the distance between start and end positions of the finger minus the distance between the start position of the finger and the target. This error was positive if the pointing movement was hypermetric and negative if hypometric. The angular error described the angle between the target and the end position of the finger, the angle vertex being the start position of the finger. This error was

positive to the left of the target and negative to the right. In addition, the variable error characterizing the distribution of the endpoint positions was calculated using the formula $SDx \times SDy \times \pi$ (Rossetti et al. 1994) for each block of nine movements made in the same experimental condition.

To explore whether the CNS sequences the trunk and arm movements to minimize trunk-motion-induced Coriolis torques (but not the centripetal and inertial interaction torques resulting from trunk motion), the timing between the onset and offset of the finger and trunk movements was analyzed for reaches to T1 and T3 (these movements involved significant trunk rotation) using the finger and trunk velocity profiles calculated in a fixed, external reference frame. The linear tangential velocity of the finger was obtained by differentiating the coordinates of the finger marker position. A threshold of 5% peak linear velocity was used to determine the onset and offset of the finger movement from the beginning of each trial. The trunk angular velocity was obtained by differentiating the angular position of the line joining the right and left shoulder markers in the horizontal plane, although slight translation (leaning) of the trunk toward the target was generally involved in addition to rotation. A 5% peak angular velocity threshold was used to identify the onset and offset of trunk movement. The finger movement onset (offset) time was subtracted from the trunk movement onset (offset) time. A positive difference indicated that the finger started (stopped) moving first in a particular trial.

Coriolis torques induced by trunk rotation are maximized when the angular velocity of the trunk and the linear velocity of the arm relative to the trunk reach their peak values simultaneously. Thus in addition to its velocity obtained in a fixed reference frame as described in the preceding text, the velocity of the finger was calculated in a reference frame moving with the trunk whose origin was located midway between the two shoulder markers. To do so, a rotation matrix and a translation vector were used to transform the finger position from fixed, external coordinates to rotating, trunk-based coordinates. Differentiation of the latter coordinates provided the linear velocity of the finger relative to the trunk. The relative asynchrony between the peak velocities of the finger and trunk was found by subtracting the time-to-peak linear relative velocity of the finger from the time-to-peak angular velocity of the trunk. Additionally, at the instant of maximum finger relative velocity, the ratio of the trunk angular velocity to the trunk peak angular velocity was calculated.

The influence of the experimental conditions on the trajectory curvature, reaching accuracy, and timing variables was tested using univariate ANOVAs for repeated measures. The repeated-measures factors were the vision condition (light and dark), speed condition (slow and fast), and target location (T1, T2, or T3). For the two targets involving significant trunk rotation (T1 and T3), additional ANOVAs were performed with trial number (1–9) as a repeated-measures factor to assess whether the trajectory curvature and/or reaching accuracy changed as movements were repeated within the same condition. Tukey's honest significant difference (HSD) test was used for post hoc comparisons. The statistical significance threshold was set at 0.05.

Inverse dynamics modeling

A simplified model of the arm/trunk system was used to compute the interaction torques at the shoulder and elbow during reaching to the three targets. The Lagrangian formulation was used to derive the equations of motion for a three-link model of the upper portion of the torso, upper arm, and forearm and hand moving in the horizontal plane (see APPENDIX). For each subject, segmental parameters were calculated using anatomical measurements and published regression equations (Chandler et al. 1975; Zatsiorsky and Seluyanov 1983, 1985). Because the arm segments were not strictly contained in the horizontal plane (shoulder abduction: ~40°), the segmental lengths were projected onto the horizontal plane, and their inertias were scaled according to each segment's mean angle with the horizontal plane. Our goal in the present paper was to estimate the size and direction of the interaction torques at the arm joints contingent on trunk motion and to assess their potential to affect the hand trajectory. Joint position, velocity, and acceleration profiles of sets of nine movements performed in the same condition were time-scaled and averaged to serve as inputs to the model. Leftward trunk rotation, shoulder and elbow flexion were considered positive, with 0° indicating a trunk parallel to the frontal plane, an upper arm colinear with both shoulders and a fully extended elbow. The interaction torque at the shoulder (or elbow) was defined as the summed contributions of Coriolis, centripetal, and inertial interaction torques dependent on elbow (or shoulder) and trunk motions.

RESULTS

Stick figures of individual reaching movements performed by one subject to each of the targets in the light-slow condition are shown in Fig. 2. In all subjects, the finger and trunk followed relatively smooth trajectories with reaching movements to T1 (Fig. 2*A*) and T2 (Fig. 2*B*) involving the largest and smallest amount of trunk rotation, respectively. Although subjects were instructed to avoid leaning toward the targets, some translation of the trunk did occur (mean displacement of midpoint of shoulder markers between start and end of reaches: 6.3, 1.6, and 2.5 cm for T1–T3, respectively).

Peak trunk and finger velocities

As subjects extended the arm and rotated the trunk to reach T1, the mean peak angular velocity of the trunk was 134 and 199°/s in slow and fast reaches, respectively (Fig. 3*A*). The

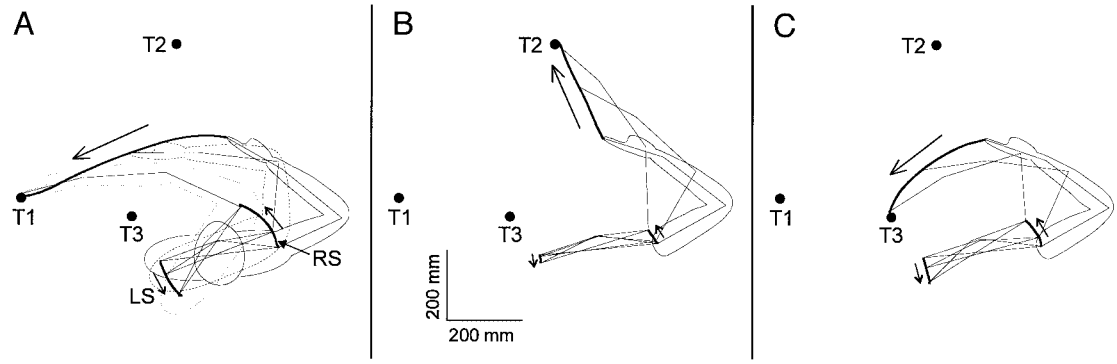

FIG. 2. Stick figures of reaching movements to targets T1 (*A*), T2 (*B*), and T3 (*C*) performed in the light-slow condition by *subject S1*. Thick lines represent the trajectory of the finger (with arrows indicating movement direction), and of markers attached to the left (LS) and right (RS) shoulder markers.

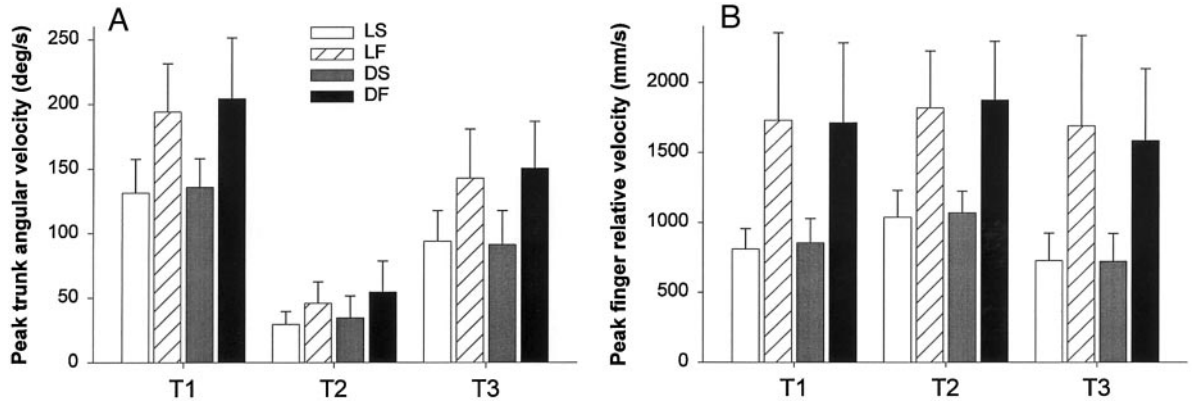

FIG. 3. Peak trunk angular velocity (*A*) and peak finger linear velocity relative to the trunk (*B*) during reaching movements to the 3 targets (T1, T2, T3) in the 4 experimental conditions (LS: light-slow, LF: light-fast, DS: dark-slow, DF: dark-fast). Each bar is the mean (±SD) of 7 subjects.

peak trunk angular velocity was significantly smaller in reaching movements to T3, which itself was greater than in movements to T2, which involved the least amount of trunk rotation [93 and 147°/s for slow and fast reaches to T3 and 32 and 50°/s for slow and fast reaches to T2, respectively; $F(1,6) = 114.87$, $P < 0.001$; Tukey HSD post hoc test, $P < 0.001$]. For all targets, the peak trunk angular velocity was ~50% greater in fast than in slow movements [$F(1,6) = 70.99$, $P < 0.001$] but was not affected by the vision condition ($P > 0.1$).

The peak value of the finger relative velocity (the velocity of the finger calculated in a trunk-based frame of reference) in fast movements was twice that in slow movements [1,736 vs. 869 mm/s; $F(1,6) = 17.62$, $P < 0.01$] but was similar under both vision conditions ($P > 0.9$; Fig. 3*B*). In slow movements, the peak velocity of the finger relative to the trunk was sensitive to target location [$F(2,12 = 36.70$, $P < 0.01$]. It was largest in reaches to T2 involving little trunk motion, followed by reaches to T1 associated with the finger moving to the left and away from the body, and finally to T3 in which the finger-to-trunk distance was kept approximately constant (mean values: 832, 1,053, and 723 mm/s for T1–T3, respectively; Tukey HSD post hoc test, $P < 0.05$). In fast movements, the peak finger relative velocity was similar for all targets (1,723, 1,847, and 1,638 mm/s for T1–T3, respectively, $P > 0.05$).

Maximal deviation of the finger trajectory in external space

The finger trajectories of reaching movements performed by one subject (*S5*) in all experimental conditions are shown in Fig. 4. Movements made by other subjects had similar finger trajectories. Observed in an external frame of reference, trajectories to the targets requiring substantial leftward trunk rotation (T1 and T3) were outwardly bowed for both visual conditions and movement speeds. In contrast, the finger trajectories of reaching movements to T2 produced mainly by rotations in the arm joints appeared relatively straight.

The maximal trajectory deviation was minimal in movements to T2 (mean: <5 mm) but increased to 55 mm in movements to T1 and T3, a statistically significant increase for both targets [$F(2,12) = 34.59$, $P < 0.0001$; Tukey HSD post hoc test, $P < 0.001$; Fig. 5]. Contrary to T1 and T3, both negative and positive values of maximal deviation were found for reaches to T2, indicating that for this target the largest trajectory deviation could occur on either side of the straight line joining the start and end positions of the finger. Increasing the reaching speed or removing visual feedback had no effect on the maximal trajectory deviation in movements to any of the targets ($P > 0.05$).

Accuracy of the reaching movements

Subjects generally overshot the target positions with a mean radial error of about 6 mm (Fig. 6*A*), a common finding for reaching to visual targets (e.g., Foley and Held 1972). Target location had an effect on the radial error [$F(2,12) = 5.33$, $P < 0.03$], but significant interactions revealed that this effect was dependent on the other factors. Without vision, movements were more hypermetric when reaching to T2 than to T3 [$F(1,6) = 7.74$, $P < 0.01$; Tukey HSD post hoc test, $P < 0.01$], but no difference occurred when vision was available ($P >$

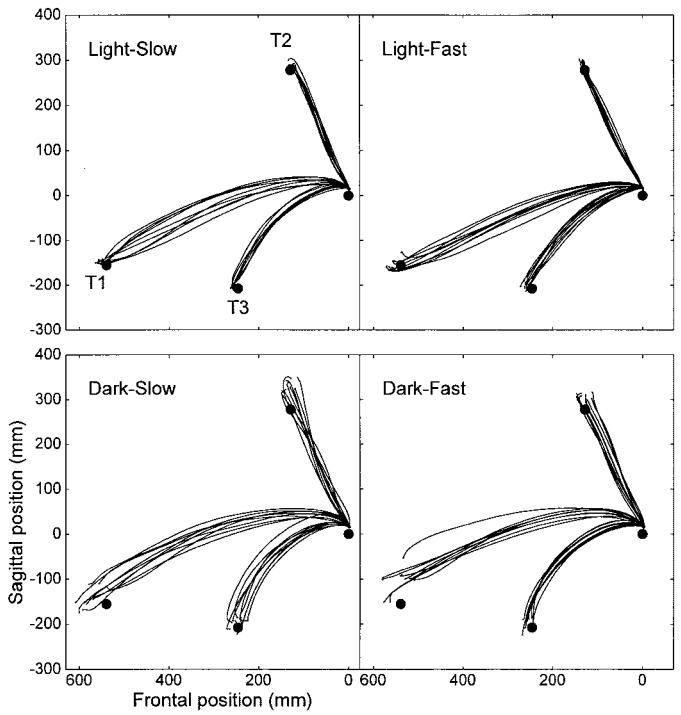

FIG. 4. Finger trajectories of reaching movements performed by *subject S5* in each experimental condition to the 3 targets (identified at *top left*).

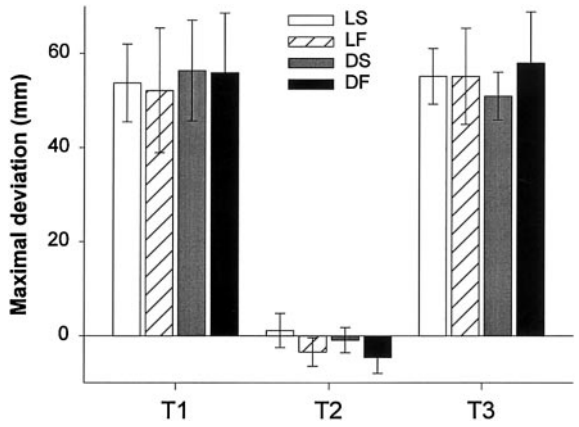

FIG. 5. Maximal deviation of finger trajectories during reaching movements to the 3 targets in the 4 experimental conditions. Rightward deviations are positive. Symbols are the same as in Fig. 3. Each bar is the mean ± SE of 7 subjects.

0.05). Similarly, in slow reaches, subjects tended to overshoot T2 while undershooting T3 [$F(1,6) = 7.55$, $P < 0.01$; Tukey HSD post hoc test, $P < 0.01$] with no significant difference for fast reaches ($P > 0.05$). In all conditions, the radial errors of movements to T1 and T2 did not differ significantly ($P > 0.05$).

For all experimental conditions, subjects generally pointed to the right of the target position (mean angular error: −2.2°; Fig. 6*B*). There were no significant main effects of the three factors on the angular error and no interactions ($P > 0.05$). However, the largest angular errors (about −4°) were associated with reaching movements performed in the dark to targets requiring substantial leftward displacement (T1 and T3). Thus when deprived of visual feedback, subjects consistently underestimated the amount of leftward trunk and arm rotation necessary to reach these targets. In contrast, angular errors in movements to T2 were small in both visual conditions (generally, between 0 and −1°).

The variable error characterizing the distribution of the endpoint positions was largest for movements to T1 (during which the hand moved a substantial distance away from the rotating trunk) than for movements to the other two targets [1,029 mm^2 for T1 vs. 296 and 388 mm^2 for T2 and T3, respectively; $F(2,12) = 63.75$, $P < 0.0001$; Tukey HSD post hoc test, $P < 0.001$; Fig. 7]. The variable error increased threefold when visual feedback was removed [from 270 to 872 mm^2; $F(1,6) = 54.77$, $P < 0.001$; compare size of symbols between *top* and *bottom* in Fig. 7] with a significant interaction indicating that the increase was larger for movements to T1. The variable error was unaffected by movement speed ($P > 0.05$).

Movement sequencing

In reaching movements to T1 and T3, both arm extension and leftward trunk rotation contributed substantially to the displacement of the hand. In general, the trunk began to move first while the position of the finger in external space remained unchanged for ~75 ms (Fig. 8, dashed and thin solid lines, respectively). The trunk and finger then moved simultaneously. For all subjects in all conditions, the trunk was the last to stop moving, on average ~425 ms after the end of the finger movement (i.e., when the finger absolute velocity decreased below threshold). During this last phase of the movement, the trunk often reversed direction (indicated by the open arrow in Fig. 8) and rotated slightly rightward (i.e., the negative portion of the trunk angular velocity profile). Thus based on the analysis of the velocity profiles in an external frame of reference, the finger movement generally occurred entirely during trunk movement with some trunk rotation occurring before and after the finger displacement.

The delay between the onsets of trunk and finger movement did not vary significantly across experimental conditions ($P > 0.05$). However, the duration of trunk movement occurring after the end of finger movement was 50% longer in reaches to T3 than to T1 [mean values of 515 and 339 ms, respectively; $F(1,6) = 92.16$, $P < 0.0001$; Table 1], 16% longer in slow than in fast movements [459 and 395 ms; $F(1,6) = 9.58$, $P < 0.03$], and 14% longer in the dark than in the light condition [455 and 398 ms; $F(1,6) = 6.63$, $P < 0.05$].

Two additional variables were examined in movements to T1 and T3 to determine whether the CNS may sequence the arm and trunk movements to minimize trunk-motion-induced Coriolis torques. The first was the delay between the peak linear velocity of the finger relative to the trunk (thick solid line in Fig. 8) and the peak angular velocity of the trunk. The delay was generally positive with a mean value of 83 ms, indicating that the finger reached its peak velocity first. Although the delay was not significantly affected by the experimental con-

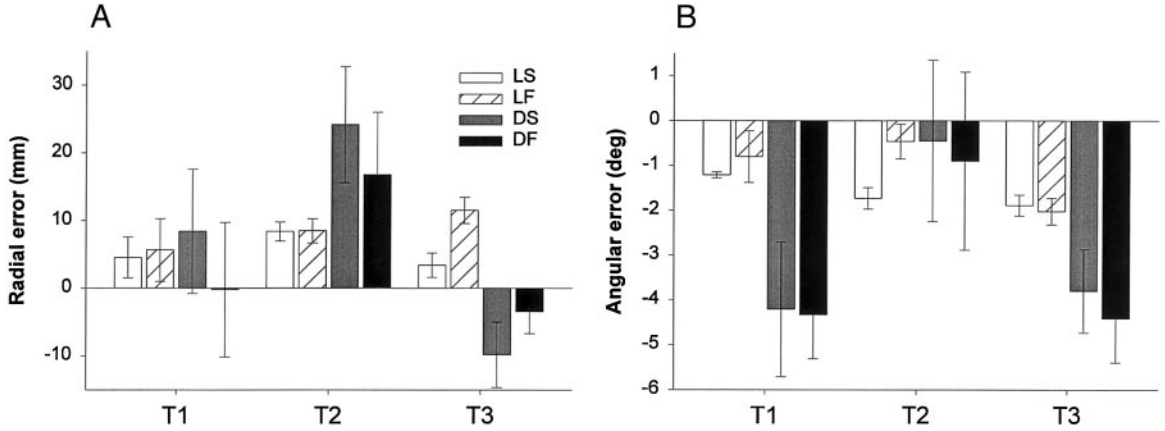

FIG. 6. Radial (*A*) and angular (*B*) errors of reaching movements to the 3 targets in the 4 experimental conditions. Errors of overshoot and leftward errors are positive. Symbols are the same as in Fig. 3. Each bar is the mean ± SE of 7 subjects.

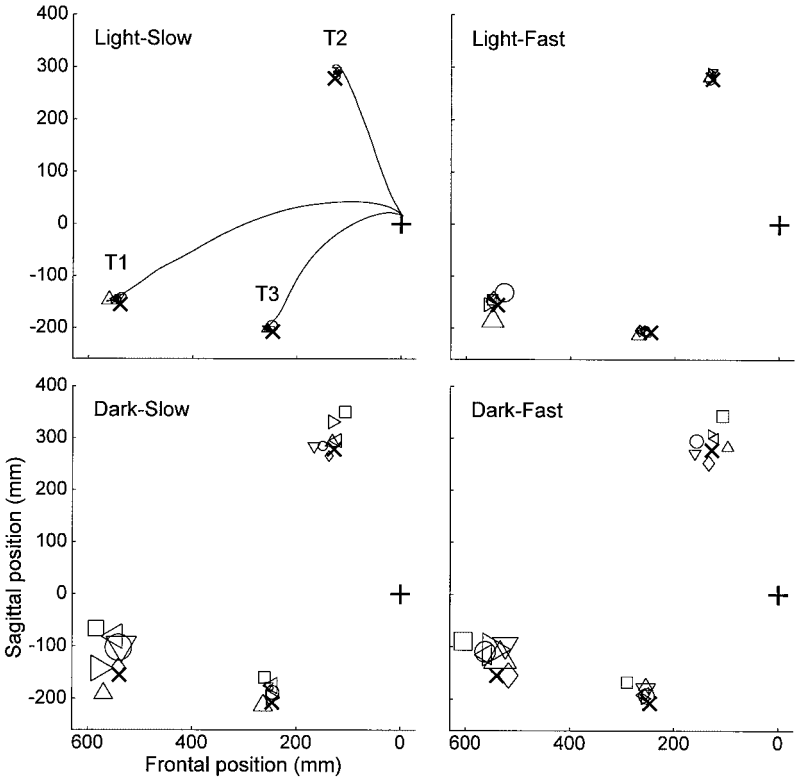

FIG. 7. Mean locations of the finger endpoint for reaching movements to the 3 targets in the 4 experimental conditions. A different symbol is used for each subject. Symbol size is scaled to the variable error values. + and ×, the start position and the locations of the targets, respectively. Sample finger trajectories to each target are shown for the light-slow condition. See Fig. 9 for 95% confidence ellipses of endpoint distributions produced by 2 of the subjects (*S1* and *S2*, represented by □ and ○ in Fig. 7).

ditions ($P > 0.05$), it tended to scale inversely with movement speed (mean delay of 103 and 64 ms in slow and fast movements, respectively; Table 1) and be shorter in reaches to T1 (mean delay of 67 and 100 ms in movements to T1 and T3, respectively). In Fig. 9, the spatial location of the finger at the times of peak linear relative velocity of the finger (+) and peak angular velocity of the trunk (▲) are indicated on the averaged finger trajectories of two subjects to the three targets in each experimental condition. The peak finger relative velocity usually occurred earlier in the trajectory, but in movements to T1, the finger occasionally reached its peak velocity after the trunk (e.g., the dark-fast trajectory performed by *S1*).

The second variable was the trunk velocity ratio, defined by normalizing the trunk angular velocity relative to its peak value at the instant of peak finger velocity in relation to the trunk. The mean ratio had a value of 0.75, indicating that, on average, the trunk velocity had reached three-quarters of its peak value when the finger was moving the fastest relative to the trunk (Table 1). Consistent with the finding of more synchronized finger and trunk peak velocities in movements to T1, the trunk velocity ratio was larger for reaches to that target (0.79) versus movements to T3 [0.72; $F(1,6) = 6.15$, $P < 0.05$]. Neither the vision nor speed condition affected the trunk velocity ratio ($P > 0.05$).

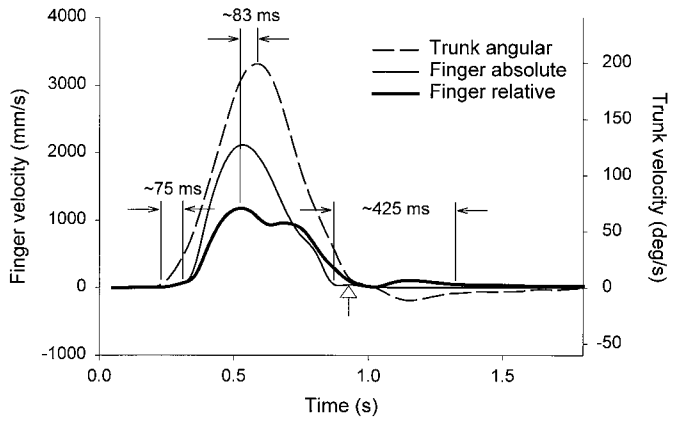

FIG. 8. Linear velocity profiles of the finger in external space (finger absolute) and relative to the trunk (finger relative) and angular velocity profile of the trunk during a single reaching movement to T1 in the light-fast condition by *subject S5*. The open arrow indicates when trunk rotation reverses direction. Note the different scales for the finger and trunk velocity profiles.

Shoulder and elbow joint torques during reaching

In Fig. 10, components of the shoulder (*top*) and elbow joint torque (*middle*) as well as shoulder, elbow, and trunk joint angles (*bottom*) are shown for slow (*3 left panels*) and fast (*3 right panels*) reaching movements to each target performed by one subject in the light condition. The same shoulder and elbow torques for fast movements are reproduced in Fig. 11 but show individual Coriolis, centripetal, and inertial interaction torque components. In both figures, flexor torques are indicated as positive and extensor torques as negative. The normal inertial torque component (Fig. 10, dashed line in *top* and *middle*) produced the required motion at the shoulder or elbow joint while the interaction torque component (Fig. 10, thin solid line in *top* and *middle*) counteracted the sum of the Coriolis, centripetal, and inertial torques arising at one joint due to motion in adjacent joints (e.g., for the shoulder, rotations at the wrist, elbow, and trunk; see individual interaction torque components for fast movements in Fig. 11). The net torque (Fig. 10, thick solid line in *top* and *middle*) represented the sum of these two components, and, in the absence of any adjacent joint motion (and thus interaction torque), the net torque would have re-

TABLE 1. *Movement sequencing variables for reaching movements*

	T1				T3			
	LS	LF	DS	DF	LS	LF	DS	DF
Delay at onset, ms	−61 ± 36	−70 ± 38	−88 ± 43	−67 ± 38	−66 ± 32	−75 ± 63	−108 ± 50	−67 ± 57
Delay at offset, ms	333 ± 98	301 ± 110	393 ± 123	327 ± 93	505 ± 122	454 ± 132	603 ± 150	497 ± 126
Peak velocity delay, ms	89 ± 100	58 ± 52	70 ± 71	49 ± 48	138 ± 37	75 ± 23	113 ± 53	75 ± 14
Trunk velocity ratio	0.75 ± 0.12	0.79 ± 0.14	0.80 ± 0.10	0.81 ± 0.13	0.71 ± 0.09	0.71 ± 0.16	0.78 ± 0.10	0.69 ± 0.15

Variables for reaching movements to the target locations T1 and T3 in 2 visual conditions (light, L; dark, D) and 2 movement speeds (slow, S; fast, F) for 7 subjects (means ± SD). Statistically significant differences are indicated in the text.

duced to the normal inertial torque. For all subjects, joint torque profiles were similar across vision conditions and also speed conditions, although scaled in amplitude and duration in the latter case.

The locations of T1 and T2 were designed to elicit similar elbow and shoulder joint rotations during the reaching movements, with and without significant trunk motion respectively. Experimentally, slightly smaller arm joint excursions were observed for T2 than T1 (Fig. 10, *bottom*), most likely because subjects relied somewhat on trunk rotation (and thus less on arm joint rotations) to reach T2. Nevertheless, the normal inertial torque profile at the shoulder and elbow joint was substantially similar for both targets in slow and fast movements (Fig. 10, compare the dashed lines in the *1st* and *2nd* and *4th* and *5th panels*, respectively, *top* and *middle*), which was consistent with our goal of comparable arm joint motions for these two targets. When subjects reached to T3, they used smaller arm joint excursions and an intermediate amount of trunk rotation (Fig. 10, *bottom*).

Despite the use of similar arm joint rotations to reach T1 and T2 at either movement speed, the interaction torque profile at the shoulder and elbow was considerably different for these two targets because of the disparity in trunk rotation involvement. For instance, early in reaching movements to T2 (involving minimal trunk motion), the elbow extension imposed a flexor torque at the shoulder which was counteracted by an initially extensor interaction torque component at the shoulder (negative portion of shoulder interaction torque, *top*, *2nd* and *5th panels*). In reaches to T1 and also to T3 (involving substantial and intermediate amounts of trunk rotation, respectively), this extensor portion disappeared and the interaction torque component produced by the shoulder had a flexor (positive) influence on the upper arm from the start of the movement (*top*, *1st*, *3rd*, *4th*, and *6th panels*). When normalized to the peak flexor normal inertial torque, the peak flexor shoulder interaction torque was generally largest for reaches to T1 followed by T2 and T3 (group values: 1.39, 1.01, and 0.98 for slow and 1.24, 1,17, and 0.86 for fast movements). These variations were largely due to sign reversals in the inertial interaction torque and to changes in the relative magnitude of the Coriolis torque across targets (Fig. 11, *top*, compare the dash-dotted and thin solid lines across targets). In particular, the Coriolis torque at the shoulder was largest for reaches to T1 (involving considerable trunk angular and hand radial displacements) and smallest for reaches to T3 (requiring little change in the hand's distance from the trunk). The mean peak shoulder Coriolis

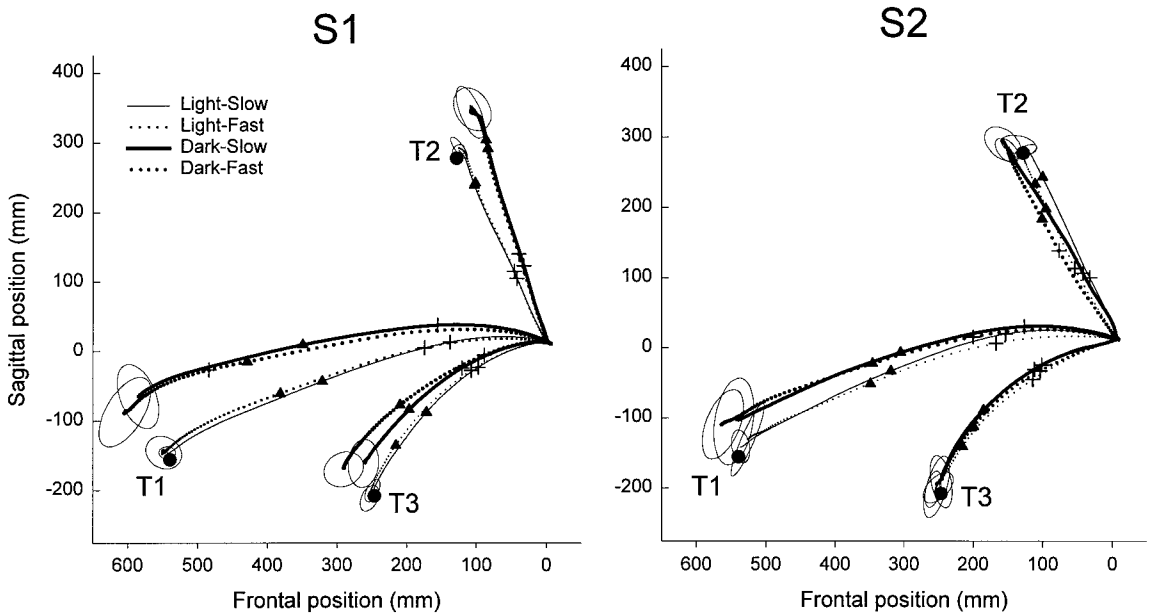

FIG. 9. Averaged finger trajectories of 2 subjects to the 3 targets in each experimental condition. The finger spatial locations associated with the times of peak linear relative velocity of the finger (+) and peak angular velocity of the trunk (▲) are indicated for all targets although the peak velocity delay and trunk velocity ratio were only calculated for targets T1 and T3 (see Table 1). For each subject and condition, 95% confidence ellipses of endpoint distributions are shown [see also □ (for *S1*) and ○ (for *S2*) variable error symbols of Fig. 7].

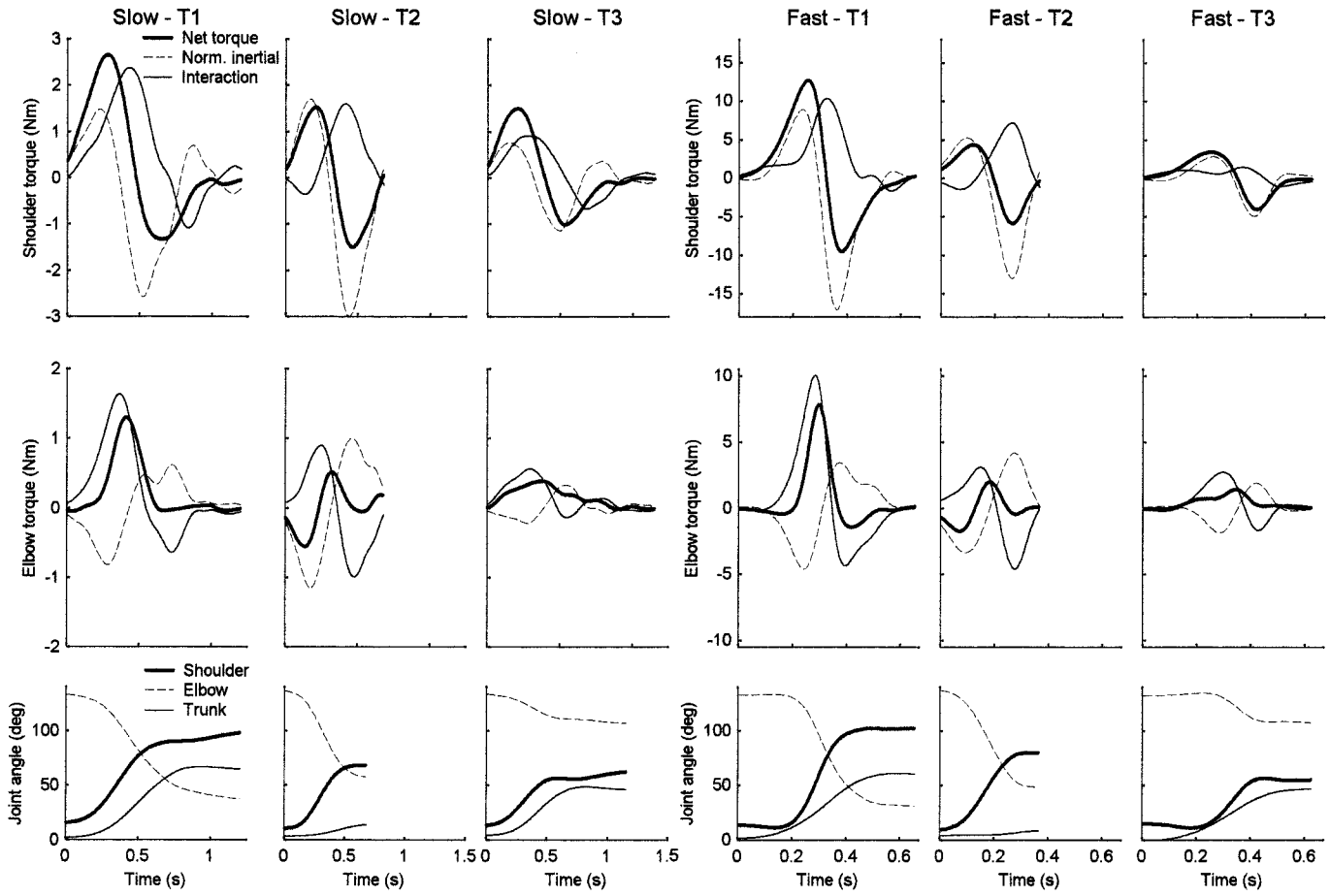

FIG. 10. Components of the shoulder (*top*) and elbow (*middle*) joint torque profiles (outputs of the simplified dynamical model), and experimentally measured shoulder, elbow and trunk joint angles (*bottom*) of slow (*3 left panels*) and fast (*3 right panels*) reaching movements to each target performed by 1 subject in the light condition. Flexor torques are positive and extensor torques are negative. The normal inertial torque component (dashed line, *top* and *middle*) produces the required motion at the shoulder or elbow joint. The interaction torque component (thin solid line, *top* and *middle*) counteracts the sum of the Coriolis, centripetal, and inertial torques arising at 1 joint due to motion in adjacent joints. The net torque (thick solid line in *top* and *middle*) represents the sum of these 2 components.

torque values were 1.83, 1.67, and 0.32 Nm for slow and 9.62, 6.25, and 2.01 Nm for fast movements to T1–T3, respectively (values normalized to peak flexor normal inertial torque: 1.11, 0.91, and 0.34 for slow and 1.20, 1.10, and 0.48 for fast movements).

At the elbow joint, the interaction torque component steadily increased its contribution to the net torque as trunk recruitment increased. When normalized to the peak flexor normal inertial torque, the peak flexor elbow interaction torque was more than twice as large in reaching movements to T3 than to T2 and three times as large in movements to T1 than to T2 (group values: 2.70, 0.87, and 2.33 for slow and 2.95, 0.89, and 2.28 for fast movements to T1–T3, respectively). During reaching movements to T1 and T3, the elbow interaction torque component was largely flexor to counteract dynamic influences from both the shoulder and trunk motions that would overextend the elbow. These influences included larger Coriolis and centripetal torque components than in movements to T2 contingent on trunk rotation (compare the thin solid and dotted lines across all targets in Fig. 11, *bottom*). For instance, the mean peak elbow Coriolis torque values were 0.69, 0.12, and 0.23 Nm for slow and 2.41, 0.35, and 0.89 Nm for fast movements to T1–T3, respectively (values normalized to peak flexor normal inertial torque: 1.06, 0.11, and 0.80 for slow and 1.01, 0.10, and 0.73 for fast movements). Consequently, the net elbow torque was almost solely flexor (positive) when the movement involved significant trunk rotation (Fig. 10, thick solid line in *middle* of *1st, 3rd, 4th,* and *6th panels*), despite the fact that the elbow needed to extend to reach all three targets. In contrast, the net elbow torque was initially extensor (negative) in reaching movements with little trunk motion (thick solid line in Fig. 10, *middle, 2nd* and *5th panels*).

In summary, when reaching movements involved simultaneous leftward trunk rotation, the shoulder and elbow joints generated additional flexor torque components to counteract the interaction torque contingent on trunk motion acting to extend the arm joints. In the experiment, movements to T1 and T2 involved similar arm joint rotations with or without significant trunk motion, respectively, thus allowing the impact of trunk rotation on each arm joint torque to be assessed. For the group, 0.54 and 2.22 Nm of additional peak flexor shoulder interaction torque was generated when subjects reached to T1 rather than T2, in slow and fast movements, respectively. At the elbow, the corresponding increase in peak flexor interaction torque was 0.79 and 4.58 Nm.

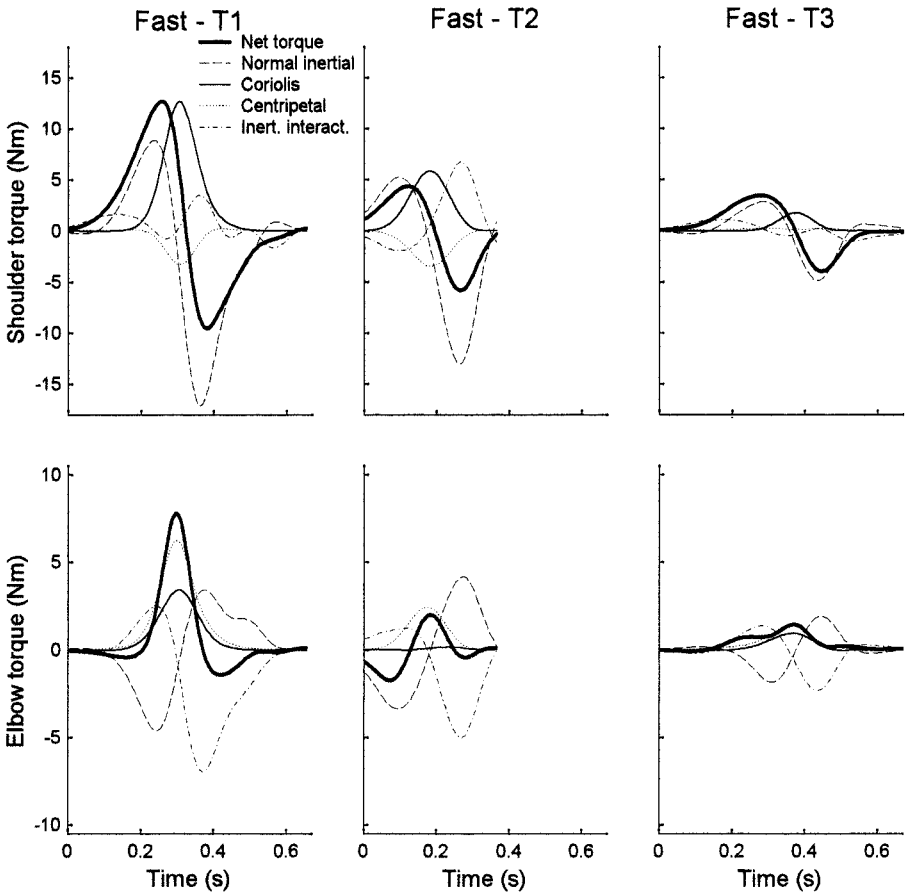

FIG. 11. Shoulder (*top*) and elbow (*bottom*) net and normal inertial torque components (also shown in Fig. 10, *3 right panels*) as well as Coriolis (thin solid line), centripetal (dashed line), and inertial interaction (dashed-dotted line) torque components of fast reaching movements to each target performed by 1 subject in the light condition.

DISCUSSION

The impetus for this study was the observation that individuals exposed to constant velocity whole body rotation initially make errors when reaching to visual targets (Lackner and DiZio 1994). Their reaches are deflected in the direction of the Coriolis forces generated on their moving arm. We asked the question how does the nervous system deal with the Coriolis and other interaction torques that would be generated if reaching movements were made during voluntary body turning? In this circumstance, the rotating torso functions analogously to the slow-rotation room in the passive rotation studies.

We evaluated four possibilities. One is that there is no compensation for voluntary turning and that errors increase in magnitude as arm and trunk velocities are increased. The second is that visual feedback is used to guide the ongoing movements. The third is that the nervous system minimizes self-generated Coriolis torques by sequencing arm and trunk motion to avoid simultaneous high velocities of the two. Finally, anticipatory motor innervations of the arm may be implemented to counteract the potentially disruptive influence of self-generated Coriolis, centripetal, and inertial interaction torques on reaching movements.

Coriolis force magnitude and reaching errors

Reaches to targets T1 and T3 both involved considerable trunk rotation but the distance of the finger from the trunk remained largely unchanged for target T3. As a consequence, peak elbow and shoulder Coriolis torques were, respectively, up to three and five times larger for movements T1 than to T3 at both movement speeds. Nevertheless, subjects were about equally accurate on these targets both in terms of radial and angular errors. Moreover, the increase in speed did not affect accuracy despite the fact that it resulted in more than three- and fivefold increases in peak elbow and shoulder Coriolis torques, respectively. Pointing to T2, which involved virtually no trunk rotation, was associated with smaller angular errors than either T1 or T3 but larger radial errors. Finger trajectories observed in external space coordinates were bowed outward for pointing to T1 and T3 and bowed outward by comparable amounts; the maximum deviations of the reaches from a straight line were not influenced by movement speed. This pattern means that self-generated Coriolis torques do not lead to disrupted movement patterns or endpoints.

Although the finger trajectories for reaches to T1 and T3 bowed outward, it should not be concluded that this resulted from uncompensated trunk-motion-induced interaction torques acting to extend the arm joints during the movements. Rather this outward curvature should be ascribed to the purely rotational nature of the trunk's contribution to the displacement of the finger [see Pigeon et al. (2003) for a description of the appearance of the finger trajectories in a trunk-based frame of reference]. When this contribution is significant (as in movements to T1 and T3), the impetus to generate straight-line hand paths in reaching movements may not be sufficient to cause the reorganization of the arm joint coordination to do so. Other authors have suggested that in some reaching tasks, the motor system may trade off the straightness of the hand path against

the computational complexity of executing the path (Haggard and Richardson 1996; Haggard et al. 1995). In addition, biomechanical constraints (e.g., the hand coming in too close proximity to the trunk) may also partly explain the outward curvature of finger trajectories involving significant trunk contribution.

Influence of target location on peak finger velocities

In slow (but not fast) reaching movements, the peak finger relative velocity was largest in reaching movements to T2, followed by those to T1 and T3. Several factors may explain the significant effect of target location on the peak finger velocities. For instance, although the arm joint rotations to reach T1 and T2 were similar, subjects generally used more elbow extension and shoulder flexion in reaching to T1 than to T2. Contrary to what was observed, this would favor larger peak finger velocities in reaches to T1 as movement speed is known to scale with movement extent (e.g., Gordon et al. 1994b). On the other hand, it has been suggested that the inertial anisotropy of the multi-segmented arm is not fully compensated in reaching movements, leading to direction-dependent variations in peak acceleration and velocity at the hand (Gordon et al. 1994a). Judging by the inertia ellipse of the upper limb computed by Gordon and colleagues (1994a) (Fig. 5*A*), reaches to T2 were most closely oriented along the axis of least inertial resistance at movement initiation. This would favor larger peak velocities in reaches to T2 than to T1 and T3. In our experiment, the extent to which these factors influenced the reaching movements may have depended on the speed condition.

Influence of visual feedback on reaching accuracy

Visual feedback had no influence on the maximum deviations of the finger trajectories in pointing to any of the targets. Removing visual feedback did increase significantly the variable error; this may reflect the poor precision of a remembered target position relative to one which is still present (Rossetti 1998) as well as the deterioration of pointing performance when vision of the hand is prevented (Rossetti et al. 1994). The larger variable errors for pointing to T1 in the dark condition may also reflect the deterioration of the precision of proprioceptive position sense, and therefore of hand localization capabilities, at distances far from the shoulder (van Beers et al. 1998). Visual feedback also had a small effect on the angular errors in pointing to T1 and T3. In the dark, the subjects tended to underestimate the amount of trunk and arm rotation necessary to get to these targets. These larger angular errors could reflect the increased complexity of a reaching task involving substantial trunk rotation or a degradation in target-encoding capabilities pursuant to the eyes and head deviating too far from their normal resting positions (Desmurget et al. 1998; Vanden Abeele et al. 1993). Furthermore, no differential effects on accuracy were present as movement speed was increased within a light or dark trial condition. This pattern means that subjects did not use visual feedback to influence their pointing behavior in the presence of a variety of self-generated interaction torques on the arm. Vision of the limb has been shown to help patients with sensory neuropathy control intersegmental dynamics during multijoint reaching movements. On the other hand, normal subjects show no improvement in movement accuracy when visual feedback is available (Ghez et al. 1995; Sainburg et al. 1993). These reports and our own findings suggest that proprioception coupled with efference monitoring provides sufficient information for the control of self-generated interaction torques.

Sequencing of arm and trunk motion

Reaching movements to targets T1 and T3 involved large rotations of the trunk. In all conditions, the trunk began to move ~75 ms prior to the onset of finger motion and outlasted the duration of finger motion, consistent with findings from previous studies of reaching movements involving the trunk (Kaminski et al. 1995; Ma and Feldman 1995; Pigeon et al. 2000; Saling et al. 1996). Nevertheless, the finger reached peak velocity relative to the trunk ~80 ms prior to the trunk reaching peak velocity. In general, the trunk was at 75% of its peak velocity when the finger attained its peak. This pattern was not affected by experimental conditions. It means that the movements were not segmented so as to minimize self-generated Coriolis torques incumbent on torso rotation. This finding may be contrasted with those from investigations of pathological populations: in particular, decomposition of elbow and shoulder joint motions [a strategy that reduces the interaction torques at the moving joint (Bastian et al. 1996)] and transient locking of the elbow joint (Sainburg et al. 1993) have been observed in slow reaching movements performed by cerebellar subjects and in "slicing" gestures performed by deafferented subjects, respectively.

Anticipatory motor compensation for self-generated interaction torques

A key feature of the present experiment is that subjects generate high-velocity reaching movements while simultaneously rotating their trunks leftward at velocities as high as 200°/s. Because the arm movement proceeds from a rotating rather than stable trunk, additional Coriolis, centripetal, and inertial interaction torques come to bear on the arm. Our modeling results reveal that these additional interaction torques act to extend the shoulder and elbow joints over most of the movement and could thus deviate the finger trajectory in a rightward direction. To counteract such influences, both joints respond with larger flexor interaction torque components. For instance, relative to its output in movements to T2, the elbow generates an additional 0.79 and 4.58 Nm of peak flexor interaction torque in slow and fast reaches to T1, respectively. If for illustrative purposes the additional interaction torques due to trunk rotation are represented by an external force applied at the center of mass of the combined forearm-hand segment, this represents an extra 0.32 and 1.88 *g* of peak lateral rightward force counteracted by the elbow joint in slow and fast reaches. Interestingly, subjects are virtually as accurate in pointing as when their trunks are stationary. This contrasts dramatically with the slow-rotation room experiments in which reaching movements made during 60°/s room rotation with as little as 0.2 *g* of Coriolis force acting on the arm resulted in large trajectory deviations and endpoints errors in the direction of the Coriolis forces generated. Other experiments have shown that reaching movement errors in this situation scale

with room velocity (Siino-Sears et al. 2000). Such a dependency was absent for our subjects making voluntary turn-and-reach movements. It should be noted, however, that subjects were allowed to practice movements to all three targets a few times prior to experimental recording to ensure that the correct speed was used for slow and fast reaching movements. In the slow-rotation room experiments, only a few trials were required for adaptation to the Coriolis force to occur (Lackner and DiZio 1994). It is thus possible that while practicing the turn-and-reach maneuvers, the subjects initially produced errors in the direction of the trunk-motion-induced interaction torques and then quickly learned to generate compensatory arm joint torques. To test this possibility, we recorded the first 10 reaching movements to T1 performed by three additional subjects in the fast condition with visual feedback. The correct speed for the movements was demonstrated by the experimenter, but the subjects were not allowed any practice trials. The average peak trunk angular velocity was 172, 234, and 221°/s on the first, second, and third movements, respectively, which was comparable to the values obtained in the main experiment (group average for all 10 reaches: 239°/s). One-way ANOVAs were performed on the maximal trajectory deviation and the radial and angular error data with trial number as the repeated-measures factor. We found no significant change in any of the variables with trial number ($P > 0.4$), suggesting that subjects did not modify their behavior during the practice trials. This finding, along with the fact that movement errors did not scale with reaching velocity despite the increasing potential for trunk motion to perturb the arm movement, points to motor innervations being planned and engaged to counteract appropriately impending self-generated interaction torques.

Studies addressing the issue of compensation for self-generated interaction torques have shown that the phasic electromyographic (EMG) activity in muscles spanning joints with constant kinematics is influenced by the characteristics of motion in adjacent joints (Almeida et al. 1995; Cooke and Virji-Babul 1995; Gribble and Ostry 1999; Koshland et al. 2000; Sainburg et al. 1995). For instance, in a step tracking task during which a constant wrist flexion was combined with progressively larger elbow extensions, muscle-activation patterns at the wrist were modified in relation to the increasing interaction torque acting at the wrist as a result of elbow motion (Cooke and Virji-Babul 1995). Similar results were obtained in studies of single- and multijoint pointing movements involving shoulder and elbow motion alone (Almeida et al. 1995; Gribble and Ostry 1999; Sainburg et al. 1995) or combined with wrist motion (Koshland et al. 2000). Moreover, the modulations of EMG activity at stationary joints contingent on the magnitude of the interaction torque were shown to occur prior to the onset of motion at adjacent joints, suggesting that they arose through feedforward rather than feedback control (Gribble and Ostry 1999).

It has been proposed that internal representations of limb dynamics within the CNS are used in the predictive compensation of forces arising from intersegmental dynamics (Beer et al. 2000; Krakauer et al. 1999; Sainburg and Kalakanis 2000; Sainburg et al. 1993, 1999; Topka et al. 1998). In a study of mechanisms underlying the control of interaction torques during reaching movements, Sainburg et al. (1999) found that once subjects adapted to reaching with a load that altered their effective forearm inertia, they produced large errors in subsequent reaches to the same target with a new load configuration. Open-looped forward simulations using the muscle torques calculated from the adapted trials predicted the initial errors in movement direction. They concluded that to control intersegmental dynamics, the nervous system uses proprioceptive information to develop an internal model of the current state of the musculoskeletal system. Deafferented patients lack the foremost sensory modality to update such a model and are thus unable to accurately time muscle actions to counter or utilize interaction torques (Sainburg et al. 1995). In these patients, vision of the limb may partially substitute for proprioception (Ghez et al. 1995; Sainburg et al. 1993). In other groups, the finding that attempted reaching by cerebellar patients does not similarly improve when visual feedback is available led to suggestions that cerebellar pathways may be involved in the implementation of an internal model (Topka et al. 1998) or may be essential in coordinating muscle activity in linked joints (Bastian et al. 1996). Both the inability to generate muscle torques that predict and compensate for interaction torques (Bastian et al. 1996, 2000) and an impairment in generating sufficient levels of phasic muscular torques (Topka et al. 1998) have been proposed to contribute to these patients' difficulties in controlling the mechanical consequences of dynamic interactions. Finally, hemiparetic patients also exhibit deficits in reaching consistent with an impaired control of interaction torques at the elbow joint, which led some authors to suggest that the frontal cortex plays a role in the representation of limb dynamics or, alternatively, that this representation degrades as a result of disuse (Beer et al. 2000).

A general proposition of the preceding studies is that, in normal subjects, the CNS engages appropriately timed and scaled muscle force patterns to compensate for self-generated interaction torques via internalized representations of limb dynamics. Two alternative viewpoints contend that the CNS does not explicitly compute compensatory time-varying forces to offset intersegmental dynamics. The first is based on an interjoint-coordination rule termed "linear synergy," which stemmed from observations that the dynamic components of the muscle torques at both the elbow and shoulder joint are related almost linearly to each other (Gottlieb et al. 1996a,b, 1997). This rule posits that during reaching movements, the CNS specifies the dynamic torque components using the same biphasic pattern scaled for load, speed, and amplitude requirements and apportioned between joints according to movement direction. Interaction torques are a subset of such torques and as such, the inability to compensate for them is read as a failure by the CNS to generate the correctly shaped and scaled dynamic muscle torques and not as a separate mishandling of intersegmental dynamics. Thus in this framework, interaction torques do not require distinct consideration by the CNS.

The second alternative viewpoint is based on the equilibrium-point (EP) hypothesis for motor control (for a review, see Feldman and Levin 1995). It suggests that appropriate changes to equilibrium shifts may underlie the compensation for external and self-generated movement dependent loads experienced during arm movements (Gribble and Ostry 2000; see also Flash and Gurevich 1997). In the two-joint planar arm model proposed by Gribble and Ostry (2000), the slope and form of shoulder and elbow control signals were adjusted iteratively based on the difference between desired and predicted joint

angles during reaching movements. Only between two and five iterations of the model were required to simulate empirical data of multijoint movements involving different interaction torques (Gribble and Ostry 1999) and performed within a velocity-dependent force field (Bhushan and Shadmehr 1999). Although the model did not require the explicit computation of compensatory muscle forces, the results suggest that the nervous system uses information about limb dynamics and external loads to adjust control signals in a predictive manner to offset movement dependent loads.

The present findings do not allow us to determine which particular scheme the CNS uses to compensate for self-generated Coriolis, centripetal, and inertial interaction torques during reaching movements involving voluntary trunk rotation. Furthermore, in addition to anticipatory control, peripheral mechanisms may also play a role in the compensation (e.g., increases in force due to afferent feedback from sudden stretches of agonist muscles, effects of the force-velocity relationship or of the passive stiffness of muscle). In future experiments, we will further explore the locus of the compensation for interaction torques by studying reaching movements produced in combination with passive trunk rotation velocity profiles that mirror the actively generated ones. However, in combination with previous results, the present findings suggest that in normal subjects, compensatory motor innervations are engaged in a predictive fashion, with control signals appropriately mapped to individual patterns of load compensation. Specifically, such compensatory signals (whether reciprocal or affecting coactivation) prevented trunk-motion-induced interaction torques from overextending the arm joints and perturbing the finger trajectory. Additional evidence supporting the conclusion of anticipatory motor compensation for self-generated interaction torques is presented in the companion paper. In particular, it describes the pattern of joint coordination associated with the reaching movement trajectories to the three targets and identifies an external frame of reference as underlying planning implementation. Finally, a third paper currently in preparation will provide an inverse dynamics analysis of the joint coordination patterns that allows an estimate of the actual physical joint torques associated with movements to the different targets.

APPENDIX

For each joint, the dynamic equation is of the form

$$\begin{array}{llll} \tau_{Net} = \tau_{Normal\ inertial} & + \tau_{Inertial\ interaction} & + \tau_{Centripetal} & + \tau_{Coriolis} \\ \tau_t = H_1\ddot{\theta}_t & + H_2\ddot{\theta}_s + H_3\ddot{\theta}_e & + h_1\dot{\theta}_s^2 + h_2\dot{\theta}_e^2 & + 2h_1\dot{\theta}_t\dot{\theta}_s + 2h_2\dot{\theta}_t\dot{\theta}_e \\ & & & + 2h_2\dot{\theta}_s\dot{\theta}_e \\ \tau_s = H_4\ddot{\theta}_s & + H_2\ddot{\theta}_t + H_5\ddot{\theta}_e & + h_3\dot{\theta}_t^2 + h_4\dot{\theta}_e^2 & + 2h_4\dot{\theta}_t\dot{\theta}_e + 2h_4\dot{\theta}_s\dot{\theta}_e \\ \tau_e = H_6\ddot{\theta}_e & + H_3\ddot{\theta}_t + H_5\ddot{\theta}_s & + h_5\dot{\theta}_t^2 + h_6\dot{\theta}_s^2 & + 2h_6\dot{\theta}_t\dot{\theta}_s \end{array}$$

Symbols:

τ = torque; $\dot{\theta}$ = angular velocity; $\ddot{\theta}$ = angular acceleration;

$s_x = \sin\theta_x$; $c_x = \cos\theta_x$; $s_{xy} = \sin(\theta_x + \theta_y)$; $c_{xy} = \cos(\theta_x + \theta_y)$;

m = mass; I = inertia; l = length;

r = distance to center of mass from proximal joint;

$$H_1 = m_a(l_c^2 + r_a^2 + 2l_c r_a c_s) + m_f(l_c^2 + l_a^2 + r_f^2 + 2l_c l_a c_s + 2l_c r_f c_{se} + 2l_a r_f c_e) + I_u + I_a + I_f$$

$$H_2 = m_a(r_a^2 + l_c r_a c_s) + m_f(l_a^2 + r_f^2 + l_c l_a c_s + l_c r_f c_{se} + 2l_a r_f c_e) + I_a + I_f$$

$$H_3 = m_f(r_f^2 + l_c r_f c_{se} + l_a r_f c_e) + I_f$$

$$H_4 = m_a r_a^2 + m_f(l_a^2 + r_f^2 + 2l_a r_f c_e) + I_a + I_f$$

$$H_5 = m_f(r_f^2 + l_a r_f c_e) + I_f$$

$$H_6 = m_f r_f^2 + I_f$$

$$h_1 = -m_u l_c r_a s_s - m_f l_c l_a s_s - m_f l_c r_f s_{se}$$

$$h_2 = -m_f l_c r_f s_{se} - m_f l_a r_f s_e$$

$$h_3 = -h_1$$

$$h_4 = -m_f l_a r_f s_e$$

$$h_5 = m_f l_a r_f s_e + m_f l_c r_f s_{se}$$

$$h_6 = -h_4$$

Subscripts:

t, trunk; s, shoulder; e, elbow; c, clavicle (l_c represents the distance between the shoulder mid-point and the right shoulder); u, upper portion of the torso; a, upper arm; and f, forearm.

P. Pigeon was supported by a Postdoctoral Research Fellowship from the Natural Sciences and Engineering Research Council of Canada.

REFERENCES

Abend W, Bizzi E, and Morasso P. Human arm trajectory formation. *Brain* 105: 331–348, 1982.

Almeida GL, Hong DA, Corcos D, and Gottlieb GL. Organizing principles for voluntary movement: extending single joint rules. *J Neurophysiol* 74: 1374–1381, 1995.

Bastian AJ, Martin TA, Keating JG, and Thach WT. Cerebellar ataxia: abnormal control of interaction torques across multiple joints. *J Neurophysiol* 76: 492–509, 1996.

Bastian AJ, Zackowski KM, and Thach WT. Cerebellar ataxia: torque deficiency of torque mismatch between joints? *J Neurophysiol* 83: 3019–3030, 2000.

Beer RF, Dewald JPA, and Rymer WZ. Deficits in the coordination of multijoint arm movements in patients with hemiparesis: evidence for disturbed control of limb dynamics. *Exp Brain Res* 131: 305–319, 2000.

Bhushan N and Shadmehr R. Computational nature of human adaptive control during learning of reaching movements in force fields. *Biol Cybern* 81: 39–60, 1999.

Bortolami SB, Pigeon P, Lackner JR, and DiZio P. Self-generated Coriolis forces on the arm during natural turning and reaching movements. *Soc Neurosci Abstr* 25: 1912, 1999.

Chandler RF, Clauser CE, McConville JT, Reynolds HM, and Young JW. Investigation of inertial properties of the human body. *AMRL Technical Report TR-74-137*, Wright-Patterson Air Force Base, Ohio, 1975.

Cooke JD and Virji-Babul N. Reprogramming of muscle activation patterns at the wrist in compensation for elbow reaction torques during planar two-joint arm movements. *Exp Brain Res* 106: 169–176, 1995.

Desmurget M, Pélisson D, Rossetti Y, and Prablanc C. From eye to hand: planning goal-directed movements. *Neurosci Biobehav Rev* 22: 761–788, 1998.

DiZio P and Lackner JR. Congenitally blind individuals rapidly adapt to Coriolis force perturbations of their reaching movements. *J Neurophysiol* 84: 2175–2180, 2000.

Feldman AG and Levin MF. The origin and use of positional frames of reference in motor control. *Behav Brain Sci* 18: 723–806, 1995.

Flash T and Gurevich I. Models of motor adaptation and impedance control in human arm movements. In: *Self-Organization, Computational Maps and Motor Control*, edited by Morasso P and Sanguineti V. Amsterdam: Elsevier North-Holland, 1997, p. 423–481.

Flash T and Hogan N. The coordination of arm movements: an experimentally confirmed mathematical model. *J Neurosci* 5: 1688–1703, 1985.

Foley JM and Held R. Visually directed pointing as a function of target distance, direction and available cues. *Percept Psychophys* 12: 263–268, 1972.

Ghez C, Gordon J, and Ghilardi MF. Impairments of reaching movements in patients without proprioception. II. Effects of visual information on accuracy. *J Neurophysiol* 73: 361–372, 1995.

Gordon J, Ghilardi MF, Cooper SE, and Ghez C. Accuracy of planar reaching movements. II. Systematic extent errors resulting from inertial anisotropy. *Exp Brain Res* 99: 112–130, 1994a.

Gordon J, Ghilardi MF, and Ghez C. Accuracy of planar reaching movements. I. Independence of direction and extent variability. *Exp Brain Res* 99: 97–111, 1994b.

Gottlieb GL, Song Q, Almeida GL, Hong D, and Corcos DM. Directional control of planar human arm movement. *J Neurophysiol* 78: 2985–2998, 1997.

Gottlieb GL, Song Q, Hong D, Almeida GL, and Corcos DM. Coordinating movement at two joints: a principle of linear covariance. *J Neurophysiol* 75: 1760–1764, 1996a.

Gottlieb GL, Song Q, Hong D, and Corcos DM. Coordinating two degrees of freedom during human arm movement: load and speed invariance of relative joint torques. *J Neurophysiol* 76: 3196–3206, 1996b.

Gribble PL and Ostry DJ. Compensation for interaction torques during single- and multi-joint limb movement. *J Neurophysiol* 82: 2310–2326, 1999.

Gribble PL and Ostry DJ. Compensation for loads during arm movements using equilibrium-point control. *Exp Brain Res* 135: 474–482, 2000.

Haggard P, Hutchinson K, and Stein J. Patterns of coordinated multi-joint movement. *Exp Brain Res* 107: 254–266, 1995.

Haggard P and Richardson J. Spatial patterns in the control of human arm movement. *J Exp Psychol Hum Percept Perform* 22: 42–62, 1996.

Hollerbach JM and Flash T. Dynamic interactions between limb segments during arm movement. *Biol Cybern* 44: 67–77, 1982.

Kaminski TR, Bock C, and Gentile AM. The coordination between trunk and arm motion during pointing movements. *Exp Brain Res* 106: 457–466, 1995.

Koshland GF, Galloway JC, and Nevoret-Bell CJ. Control of the wrist in three-joint arm movements to multiple directions in the horizontal plane. *J Neurophysiol* 83: 3188–3195, 2000.

Krakauer JW, Ghilardi MF, and Ghez C. Independent learning of internal models for kinematic and dynamic control of reaching. *Nat Neurosci* 2: 1026–1031, 1999.

Lackner JR and DiZio P. Rapid adaptation to Coriolis force perturbations of arm trajectory. *J Neurophysiol* 72: 299–313, 1994.

Ma S and Feldman AG. Two functionally different synergies during arm reaching movements involving the trunk. *J Neurophysiol* 73: 2120–2122, 1995.

Morasso P. Spatial control of arm movements. *Exp Brain Res* 42: 223–227, 1981.

Pigeon P, Bortolami SB, DiZio P, and Lackner JR. Arm reaching movements during voluntary trunk rotation involve compensation for self-generated Coriolis forces. *Soc Neurosci Abstr* 25:1912, 1999.

Pigeon P, Bortolami SB, DiZio P, and Lackner JR. Coordinated turn-and-reach movements. II. Planning in an external frame of reference. *J. Neurophysiol* 89: 290–303, 2003.

Pigeon P, Yahia LH, Mitnitski AB, and Feldman AG. Superposition of independent units of coordination during pointing movements involving the trunk with and without visual feedback. *Exp Brain Res* 131: 336–349, 2000.

Rossetti Y. Implicit short-lived representations of space in brain damaged and healthy subjects. *Conscious Cognit* 7: 520–558, 1998.

Rossetti Y, Stelmach G, Desmurget M, Prablanc C, and Jeannerod M. The effect of viewing the hand prior to movement onset on pointing kinematics and variability. *Exp Brain Res* 101: 323–330, 1994.

Sainburg RL, Ghez C, and Kalakanis D. Intersegmental dynamics are controlled by sequential anticipatory, error correction, and postural mechanisms. *J Neurophysiol* 81: 1045–1056, 1999.

Sainburg RL, Ghilardi MF, Poizner H, and Ghez C. Control of limb dynamics in normal subjects and patients without proprioception. *J Neurophysiol* 73: 820–835, 1995.

Sainburg RL, Poizner H, and Ghez C. Loss of proprioception produces deficits in interjoint coordination. *J Neurophysiol* 70: 2136–2147, 1993.

Saling M, Stelmach GE, Mescheriakov S, and Berger M. Prehension with trunk assisted reaching. *Behav Brain Res* 80: 153–160, 1996.

Siino-Sears V, DiZio P, and Lackner JR. Rotation velocity influences the magnitude of deviations of arm reaching movements. *Soc Neurosci Abstr* 26: 63.5, 2000.

Topka H, Konczak J, Schneider K, Boose A, and Dichgans J. Multijoint arm movements in cerebellar ataxia: abnormal control of movement dynamics. *Exp Brain Res* 119: 493–503, 1998.

van Beers RJ, Sittig A, and Denier van der Gon JJ. The precision of proprioceptive position sense. *Exp Brain Res* 122: 367–377, 1998.

Vanden Abeele S, Delreux V, Crommelinck M, and Roucoux A. Role of eye and hand initial position in the directional coding of reaching. *J Mot Behav* 25: 280–287, 1993.

Wang J and Stelmach GE. Coordination among the body segments during reach-to-grasp action involving the trunk. *Exp Brain Res* 123: 346–350, 1998.

Zatsiorsky VM and Seluyanov VN. The mass and inertia characteristics of the main segments of the human body. In: *Biomechanics VIII-B*, edited by Matsui H and Kobayashi K. Champaign, IL: Human Kinetics, 1983, p. 1152–1159.

Zatsiorsky VM and Seluyanov VN. Estimation of the mass and inertia characteristics of the human body by means of the best predictive regression equations. In: *Biomechanics IX-B*, edited by Winter DA, Norman R, Wells RP, Hayes KC, and Patla AE. Champaign, IL: Human Kinetics, 1985, p. 233–239.